

SELF-ASSESSMENT OF FINITE ELEMENT SOLUTIONS APPLIED TO TRANSIENT PHENOMENA IN SOLID CONTINUUM MECHANICS

Miloslav Okrouhlík*, Svatopluk Pták*, Urmás Valdek**

The presented study evolved from authors' considerations devoted to expected credibility of results obtained by finite element methods especially in cases when comparisons with those of experiment are not available. Thus, assessing the validity of numerical results one has to rely on the employed method of the solution itself. Out of many situations which might be of importance, we paid our attention to comparison of results obtained by different element types, two different time integration operators, mesh refinements and finally to frequency analysis of the loading pulse and that of output signals expressed in displacements and strains obtained by solving a well defined transient task in solid continuum mechanics. Statistical tools for the quantitative assessment of 'close' solutions are discussed as well.

Keywords: stress wave propagation, finite element method, validity of models, accuracy assessment

Motivation

The presented paper is a part of the study dedicated to the assessment of the energy flux through a drilling bar with four spiral slots subjected to an axial impact. The problem, initially suggested by people from Sandvik Company in Sweden, is fully treated in [10] and in another paper just being prepared. The question was to find out what part of input energy, due to the axial impact, could be transferred into the energy associated with torsional displacements, which was thought to improve the rock drilling efficiency.

Authors solved the presented problem by means of FE analysis and by experiment. The FE analysis was fully three dimensional, while the experimental one relied on the surface strain measurement complemented by evaluation of measured data based on 1D wave theory for axial and torsional waves.

Before assessing the final goal, i.e. the evaluation of the energy flux at each cross section of the tube as a function of time and assessing its dependence on four different geometries of spiral slots and on the 'time length' of the input pulse, authors deemed necessary to analyze the credibility of both numerical and experimental approaches.

The analysis of FE and experimental results presented in this paper is based on the rather simple and expectable pattern of stress waves propagation through the first part of the tube for small times, i.e. before the incoming wave reaches the spiral slot. The details about the solved case and about the experiment are in [10] and will be published later. In this paper the main attention is devoted to particulars of self-assessment of finite element technology.

* prof. Ing. M. Okrouhlík, CSc., Ing. S. Pták, CSc., Institute of Thermomechanics

** Dr. U. Valdek, PhD, Ångström Laboratory, Uppsala University

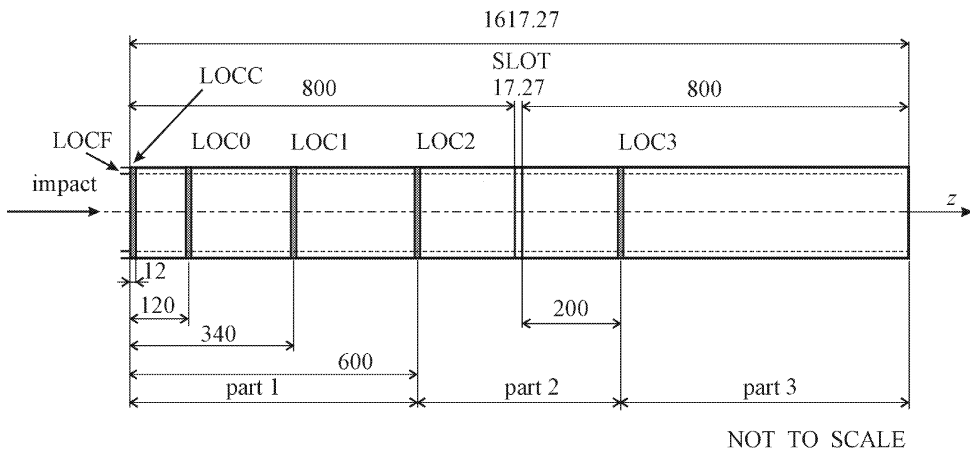
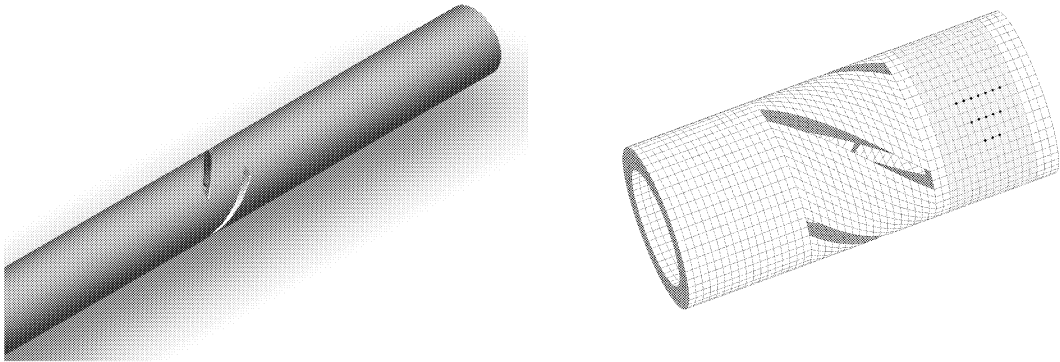


Fig.1: Tube with four spiral slots, a part of mesh assembly, tube dimensions in [mm], positions of locations where the comparison of FE and experimental data was performed

Authors believe that the discussion about the validity of these particular results is of methodical nature and might be of interest of both finite element and experimental community.

List of principal variables

$c_0 = \sqrt{E/\rho}$	speed of 1D longitudinal waves
$c_L = \sqrt{(2G + \lambda)/\rho}$	speed of longitudinal waves in unbounded 3D continuum
$c_T = c_S = \sqrt{G/\rho}$	speed of transversal (shear) waves and of 1D torsional waves
E	Young modulus
f	cyclic frequency
g	gravitational acceleration
$G = E/[2(1 + \mu)]$	shear modulus
h	mesh size
l	length
m	mass
p	pressure
r	radius
t	time

T	period
β, γ	Newmark coefficients
$\lambda = \mu E / [(1 + \mu)(1 - 2\mu)]$	Lamé's constant
μ	Poisson's ratio
ϱ	density
\mathbf{M}, \mathbf{K}	mass and stiffness matrices
$\mathbf{V}, \mathbf{\Lambda}$	modal and eigenvalue matrices
$\mathbf{q}(t), \ddot{\mathbf{q}}(t)$	displacement and acceleration arrays, functions of time
$\mathbf{P}(t)$	loading vector, function of time

1. Introduction

Assessing results of finite element (FE) analysis one is contemplating their reliability, credibility, accuracy, validity, etc. That prompts questions as: Are the results correct and/or precise? In what sense? If the results are compared with those obtained by alternative approaches, what is an acceptable agreement of different solutions? How such an agreement could be quantified?

The aim of this paper is to present a few self-checking tools allowing to assess the credibility of the FE analysis. A few study cases, on which examples of self-assessment analysis will be shown, come from the field of transient stress wave propagation in solids.

At least three reasons might be shown for this choice.

First, solving the linearly elastic stress wave propagation problems in solid continuum mechanics is a well defined task based on equations of motion, strain-displacement relations and on constitutive equations, attributed to Navier, Cauchy, Lamé, Rayleigh and others, that are known for more than 150 years. See [1].

Second, available analytical solutions of equations governing the stress wave propagation provide useful benchmark limits that could be used in the validation process of approximate numerical approaches. See [2], [3], [4], [5].

Third, the FE method seems to be most frequently employed for solving stress wave propagation tasks both in engineering and basic research. The origin of FE method goes back to the thirties of the last century when Collar and Duncan conceived aeroelasticity principles in discrete matrix expressed forms. See [6], [7]. The major steps in evolution of the FE method are vividly described in [8].

Still, both the numerical and analytical approaches to the solution of transient stress wave computation in solid continuum mechanics are far from being trivial. They require a considerable amount of pre- and post-processing activities, powerful computer resources as well as a thorough assessment of obtained results, since it is not always easy to distinguish the manifestations of Mother Nature from contributions of the side effects evoked by the various modeling approaches.

Model is a purposefully simplified concept of a studied phenomenon invented with the intention to predict what would happen if Accepted assumptions (simplifications) thus specify the validity limits of the model and strictly speaking the model is neither true nor false. And the FE method can be considered as one of models of continuum. Regardless of being simple or complex, the model is acceptable if it is applied within its validity limits and if it is experimentally approved. See [9].

The results of any experiment, however, are biased by systematic errors, noise, observational thresholds, cut-off frequency limits, etc.

Furthermore, in most cases the experimental results are not available when needed and thus the direct comparison of FE and experimental results cannot be provided. So assessing the validity of numerical results, we have to rely on what the employed numerical methods spill on themselves.

2. Benchmark studies

In this paragraph there are five cases studied in detail. As a vehicle for assessing the validity and credibility of FE modeling we will present and analyze different approaches to the FE treatment of the propagation of elastic stress waves in a tube being subjected to impact axial loading. For more details see [10]. Equations describing the propagation of undamped elastic stress waves are well known and can be found in numerous references as in [2], [3], [20]. For the FE treatment of this task the reader might refer [13], [14], [15], [16], [18], [24].

Details concerning the FE modeling allied to this case are in paragraph 2.1.

2.1. Finite element details

Geometry

An in-house finite element code called PMD (Package for Machine Design) was employed. The program, originated at seventies of the last century, is being maintained and developed by the Institute of Thermomechanics. See [24].

The tube being modeled has inner and outer radii 8 and 11 mm, respectively. Its length varies but it is always substantially ‘longer’ than the loading pulse. Tube is assembled by 3D eight-node brick elements and alternatively by four-node square axisymmetric elements. The mesh assembled out of approximately 1 mm elements is called standard (also coarse or mesh1) in the text. Finer meshes denoted mesh2 to mesh4 are considered as well. The higher numbered mesh is twice as fine as the previous one. A typical layer of standard 3D and of standard axisymmetric elements, of which the tube is assembled, is sketched in Fig. 2.

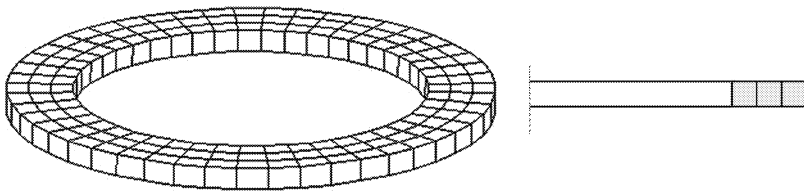


Fig. 2: Standard mesh; one layer of 3D and axisymmetric elements

Element properties

Trilinear brick eight-node elements and bilinear four-node axisymmetric elements are used. Gauss quadrature of the third order is employed in both cases.

Material properties

$$E = 2.05 \times 10^{11} \text{ Pa}, \mu = 0.24, \rho = 7800 \text{ kg m}^{-3}.$$

Loading

One side of the tube is loaded by uniform pressure, whose time dependence is given by a rectangular pressure pulse. This way, the non-linear contact problem is approximated by a simplified linear procedure. The validity of this approach is discussed in [10]. The other end of the tube is fixed.

Computational considerations

To work with ‘reasonable’ values of pressure, and to have a chance to compare the FE results with those of experiment, we could use approximations valid for 1D stress wave propagation. See [10]. Let a 1D bar be loaded by a striker falling from the height $h = 1$ m. It is assumed that the striker is of the same material as the bar and has the same cross sectional area. Its velocity, just before the impact, is $v = \sqrt{2gh} = 4.42944$ m/s. The material particle velocity of the impacted face, immediately after the impact, is $v_p = v/2 = 2.2147$ m/s. The resulting pressure, according to Young’s classical formula, see [20], is $p = E v_p/c_0 = 88.5198$ MPa, where, the 1D velocity c_0 was defined above. The time of the pulse is related to the assumed length of the striker by $t_{\text{imp}} = 2 l_{\text{striker}}/c_0$. For a hypothetical striker with $l_{\text{striker}} = 40$ mm the time length of the pulse is 15.6 microsec. Assuming the lossless impact the input energy of the bar is equal to the kinetic energy of the striker just before the impact, i.e. $m_{\text{striker}} v^2/2 = 0.548086$ J.

FE technology

Newmark time step operator (no algorithmic damping, i.e. $\gamma = 0.5$, $\beta = 0.25$, see [18]) was used with the consistent mass matrix, while the central difference operator was systematically used with the diagonal mass matrix. The time step value was evaluated from the condition that two timesteps are required for 1D longitudinal wave (taking approximate speed $c_0 = 5000$ m/s) to pass through the length of the smallest element. See [23]. In the case of the coarse mesh (mesh1) the dimensions of all elements are about 1 mm so the basic timestep = 10^{-7} s. This way, the employed timestep is one half the critical step as defined in [25], and suits well to both time step operators. Unless stated otherwise, the coarse mesh results are presented in the text.

2.2. Study case 1 – strain distributions of the same task obtained by Newmark (NM) and central difference (CD) operators

Several time marching operators for solving the systems of ordinary differential equations, suitable for the FE modeling of transient tasks of solid continuum mechanics, are known today. The detailed description of their background and analyses of their properties can be found, e.g., in [13], [16], [18]. Commercial FE packages offer plethora of approaches, see [14], [15]. The outlines and rules for their ‘safe’ usage are generally advocated; nevertheless it still might be of interest to analyze in detail the minute differences obtained by applying different integration methods to the same task.

Let’s concentrate our attention to the comparison of results obtained by Newmark (NM) and central difference (CD) methods.

The NM method is a classical representative of implicit methods. Used with consistent mass matrix and without algorithmic damping it conserves energy and is unconditionally stable. In order to minimize the temporal and spatial discretization errors the NM method is recommended, see [13], to be used with consistent mass matrix formulation.

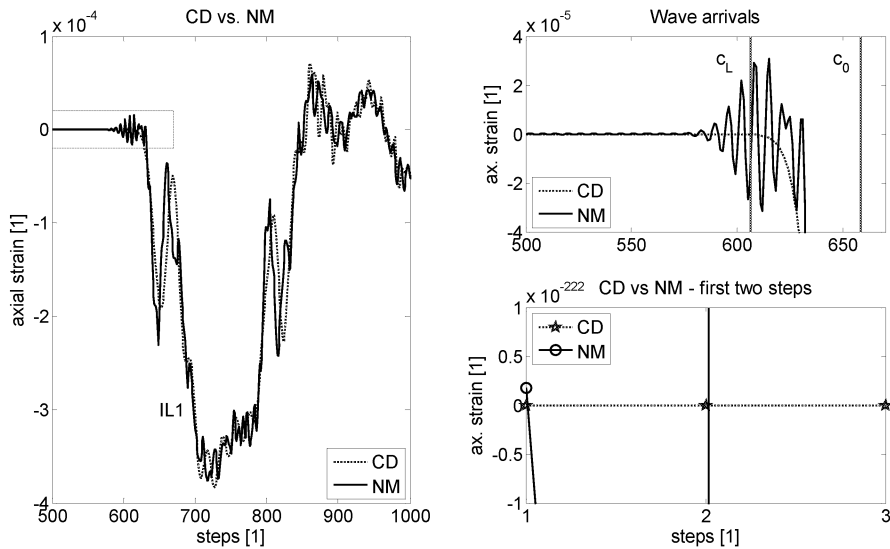


Fig.3: Time distributions of surface axial strains obtained by NM and CD operators

The CD method, the representative of explicit methods, is only conditionally stable. When used within its stability limits with consistent mass matrix formulation it also fully conserves energy. To reduce the temporal and spatial discretization errors the CD method is recommended, see [13], to be used with diagonal (lumped) mass matrix formulation. Using it with a consistent mass matrix is possible but practically prohibitive for two reasons. First, the problem becomes computationally coupled. Second, the data storage demands for the consistent mass matrix are substantially higher than those needed for a diagonal mass matrix. Today, the CD method is almost exclusively used with the diagonal mass matrix formulation, which is furthermore plausible from the point of view of minimization of dispersion effects. But using the CD method with diagonal mass matrix we are punished a little bit by the fact that the time dependence of total mechanical energy slightly fluctuates around its ‘correct’ value. See [17].

Comparison of the time history of axial surface strains at a location, whose distance from the impacted face of the tube is 340 mm, see Fig. 1, obtained by NM and CD methods using 3D elements, is presented in Fig. 3. The same time integration step ($1e-7$ [s]) was used in both cases. The proper choice of the time step value is discussed in [25]. For the NM method the consistent mass matrix was employed, while the diagonal mass matrix was used for the CD method.

The left-hand subplot presents the axial strains as functions of timesteps in the above mentioned location. The negative peak, denoted IL1, corresponds to the immediate position of the loading pulse. There is a visible difference between NM and CD results, which – from the engineering point of view – seems to be small. Often, the differences are viewed by the prism of the plotting scale. We will treat this subject in more detail in the paragraph 2.6.

In the upper right-hand subplot of Fig. 3, which is the enlarged view of the small rectangle presented on the left-hand side of Fig. 3, the theoretical positions of arrivals of hypothetical 3D (c_L) and 1D (c_0) longitudinal waves are indicated by vertical lines. Of course in a bounded 3D body no pulse, being composed on infinitely many harmonics, can propagate by any of above mentioned velocities. But the theoretical wave speeds are useful bounds for our

expectations. The detailed strain distributions, obtained by NM and CD methods, are shown as well. From the analysis of dispersion properties of finite elements and that of time integration methods, presented in detail in [13], it is known that the computed speed of wave propagation for the CD approach with diagonal mass matrix underestimates the actual speed, while using the NM approach with consistent mass matrix the actual speed is overestimated. The presented results nicely show this. When looking at the enlarged details of the wave arrivals, as modeled by NM and CD operators, a nagging question might intrude our minds. Where or actually when does the incoming pulse start? A similar subject was analyzed on experimentally obtained data in [10], where it was shown how the ‘detected’ moment of arrival depends on the observational threshold. Different frequency contents of both signals, as well as a more detailed analysis of CD and NM operators will be treated in paragraphs 2.4 and 2.5 respectively.

Less known is the fact that the speed of propagation, modeled by NM method with consistent mass matrix formulation, is actually ‘infinitely’ large. See [17]. A brief explanation of this curiosity could be sketched followingly.

Interlude – assessment of ‘variable computational speeds’ of wave propagation by analyzing two time marching algorithms for the numerical integration of the system of ordinary differential equations $\mathbf{M} \dot{\mathbf{q}} + \mathbf{K} \mathbf{q} = \mathbf{P}(t)$

The central difference (CD) method and the Newmark (NM) method lead to the repeated solutions the system of algebraic equations

$$\frac{1}{\Delta t^2} \mathbf{M} \mathbf{q}_{t+\Delta t} = \tilde{\mathbf{P}}_t, \quad (\text{a}) \quad \hat{\mathbf{K}} \mathbf{q}_{t+\Delta t} = \hat{\mathbf{P}}_{t+\Delta t}, \quad (\text{b})$$

where the effective loading forces and the effective stiffness matrix are

$$\tilde{\mathbf{P}}_t = \mathbf{P}_t - \left(\mathbf{K} - \frac{2}{\Delta t^2} \mathbf{M} \right) \mathbf{q}_t - \frac{1}{\Delta t^2} \mathbf{M} \mathbf{q}_{t-\Delta t}, \quad \hat{\mathbf{P}}_{t+\Delta t} = \mathbf{P}_{t+\Delta t} + \mathbf{M} (c_1 \mathbf{q}_t + c_2 \dot{\mathbf{q}}_t + c_3 \ddot{\mathbf{q}}_t),$$

$$\hat{\mathbf{K}} = \mathbf{K} + \frac{1}{\beta \Delta t^2} \mathbf{M}.$$

Definition of constants appearing above and more details are in [18].

Generally, the matrices \mathbf{K} , \mathbf{M} , $\hat{\mathbf{K}}$ are sparse. Nevertheless their inversions \mathbf{K}^{-1} , \mathbf{M}^{-1} as well as $\hat{\mathbf{K}}^{-1}$ (needed for extracting the displacements $\mathbf{q}_{t+\Delta t}$ at the next time step from equations (a) and (b)) are full. From it follows that in both systems of equations the unknowns are coupled. This means that when calculating the i -th displacement, there are all other displacements, which – through the non-zero coefficients of a proper inverse matrix – are contributing to it.

Thus, when (at the beginning of the integration) a nonzero loading is applied at a certain node, then (at the end of the first integration step) the displacements at all nodes of the mechanical system are non-zero, indicating that the whole system already ‘knows’ that it was loaded, regardless of the distance between the loading node and the node of interest.

The magic spell could only be broken if the matrix, appearing in the system of algebraic equations, is diagonal, because its inversion is then diagonal as well. This, however, could only be provided for the CD approach, operating with mass matrix, because it is the mass matrix only which can be meaningfully diagonalized. See [18].

End of interlude.

The above discussion is illustrated in the lower right-hand side subplot of Fig. 3 where one can see the strains computed by CD and NM operators (at a location whose distance from the loading area is 340 mm) during the first three steps of integration. The CD operator, with a diagonal mass matrix, gives the expected series of pure zeros, while the NM method gives values negligibly small (of the order of 10^{-222}) but still non-zero. It should be emphasized that this has nothing to do with round-off errors. The same phenomenon would have appeared even if we had worked with symbolic (infinitely precise) arithmetics.

The computed value of speed of stress wave propagation (obtained by the registration of the first non-zero response at a certain time in a given distance from the loading point using the NM method) depends not only on the distance of the point of observation from the loading node but paradoxically on the timestep of integration as well. The CD method spares us of these troubles.

And now it is the *computational threshold* which enters our considerations. It depends on the number of significant digits used for the mantissa representation of the floating number. See [19].

The minimum floating point number that can be represented by the standard double precision format (that we have used for the computation) is of the order of 10^{-308} . This is our numerical observational threshold allowing distinguishing the value 10^{-222} in the first step of the lower right-hand side of Fig. 3.

If, for the same numerical integration in time, we had employed the single precision format (threshold of the order of 10^{-79}) we would have observed pure zero in the first step instead and the first non-zero value would appear later.

Of course, nobody would measure the wave speed this way. What would be a common sense approach? Sitting at a certain observational node, whose distance from the loaded node is known, one would estimate the speed by measuring the time needed for the arrival of the ‘measurable’ or ‘detectable’ signal.

And the measurable signal is such that is in absolute value greater than a ‘reasonable’ *observational threshold*. And what is a proper value of it is a good question.

A thought experiment accompanied by FE computation might help. Imagine a standard finite element double-precision computation giving at a certain time the spatial distribution of displacements at a node on the surface of a body. Assume that the distance of our observational node from the loading node is known. Now, let’s set a ‘reasonable’ value of the threshold and apply a sort of numerical filter on obtained displacements, which erases all the data whose absolute values are less than the mentioned value of the threshold. This way, for a given threshold value, we get a certain arrival time and from the known distance we obtain the propagation speed. Working with displacements normalized to their maximum values allows us to consider the threshold values as the relative ones. For more details see [17].

Varying the simulated threshold value in the range from 10^{-6} to 10^{-1} we will get a set of different velocities of propagation. As a function of threshold they are plotted in Fig. 4. Material constants for the standard steel were used. The horizontal lines represent the theoretical speeds for longitudinal waves in 3D continuum, for longitudinal plane stress waves in 2D continuum as well as for the shear waves. Obviously, the shear wave speeds are identical both for 3D and 2D cases. See [2], [20].

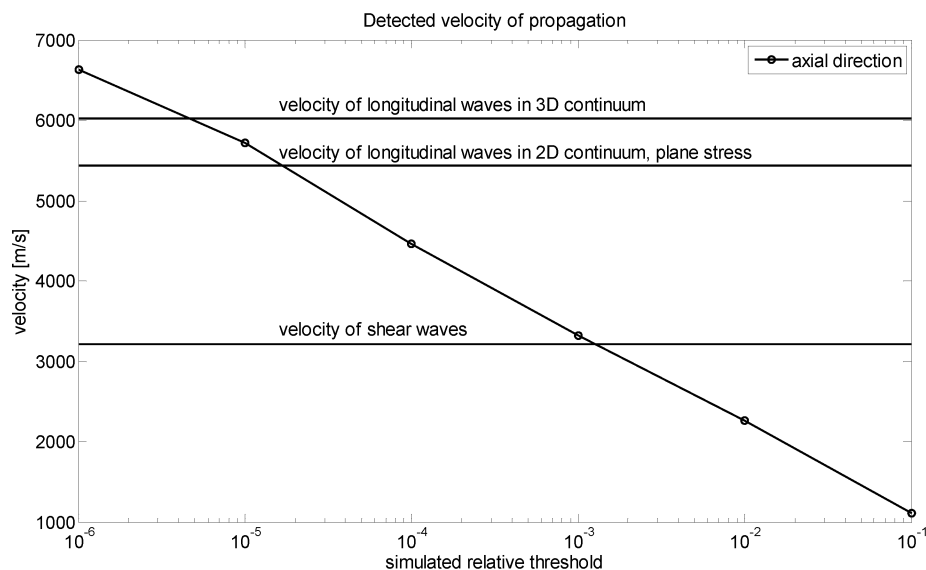


Fig.4: Detected velocity of propagation vs. relative threshold

The previous discussion might appear rather academic. The threshold issue, however, is really important when the speed of propagation is being determined by experimental means. The procedure is the same as in the numerical simulation approach. Observing the first ‘measurable’ response at a certain time in a given distance from the loading point one can estimate the speed of propagation. As before, the estimated velocity value depends on the observational threshold value. There is, however, a significant difference. While we could almost arbitrarily vary the simulated threshold value in the numerical treatment, the value of observational threshold is usually constant for the considered experimental setup being used for the measurement of a particular physical quantity.

It is known that the longitudinal waves carry substantially less amount of energy than these of the shear and Rayleigh waves and that the surface response, measured in displacements or strains, is of substantially less magnitude for the former case.

From the experimental point of view one can conclude that for a correct capturing of the longitudinal velocity value, the relative precision of at least of the order of 10^{-6} is required. This is a tough request. The relative threshold of the order of 10^{-3} is more common in experimental practice. However, in an experiment with the relative precision of the order of 10^{-3} , one would not detect the arrival of longitudinal waves and might wrongly conclude that the first arriving waves are of the shear nature or would estimate the velocity of propagation of the order of 3000 m/s.

All this fuzz is about the margins of our ability to distinguish something against nothing. This is, however, crucial for any meaningful human activity.

2.3. Study case 2 – strain distributions of the same task obtained by 3D and axisymmetric elements

Another check of validity of FE analysis might be based upon analyzing the results of the transient modeling of the above mentioned tube modeled by eight-node 3D elements

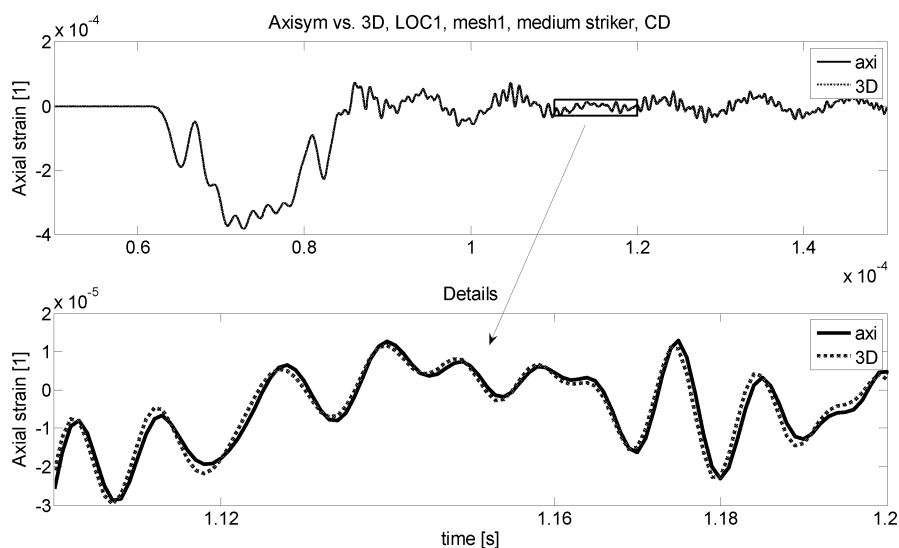


Fig.5: Comparison of axial strains obtained by 3D and axisymmetric elements

and 4-node bilinear axisymmetric elements with diagonal mass matrix formulations. The central difference method (CD) with constant `timestep = 1e-7 [s]` was employed. For more details see [10].

Axial strains at a certain surface location computed by both time operators are plotted in Fig. 5. The differences of solutions obtained by two different element types are almost undistinguishable. We know, however, that distinguishability is a matter of the employed plotting scale as one can see in the lower part of Fig. 5. In this particular case, the differences between close solutions, quantitatively expressed by means of relative errors based on the centred correlation coefficient, which has a nice geometrical interpretation as a cosine of an angle between two vectors (a signal is considered as the n -dimensional vector in time as described in [27]), are as follows.

	Radial displacements	Axial displacements	Axial strains
$\cos(\text{fi})$	9.999737901746213e-001	9.999999591806313e-001	9.997847497832014e-001
with following relative differences	2.620982537870908e-005	4.081936866295877e-008	2.152502167985793e-004

Having small differences between two alternative approaches does not automatically imply that the results are correct. It only means that for a given loading and the employed time and space discretizations, there is almost no ‘measurable’ difference between results obtained by two types of approaches. One has to realize that the existence of close solutions, stemming from alternative approaches, is only a necessary, but not a sufficient, condition of ‘correctness’. And what is ‘correct’, in the sense of correct modeling the Mother Nature, is difficult to define.

2.4. Study case 3 – comparison with experiment

In the upper part of Fig. 6 the FE axial strains at a certain location on the outer surface, whose distance from the loading face is 340 mm, are compared with those obtained experimentally. The FE analysis was carried out by 3D elements with consistent mass matrix. The

NM method (no algorithmic damping) with timestep $1e-7$ s was used. The experimental data were obtained by 3 mm strain gauges glued in the middle part of the above mentioned location. The standard bridge to eliminate bending effects with a digital recorder having the sampling rate 1 MHz was employed. The used 16-bit amplifier with shunt calibration had the upper cut-off frequency 0.1 MHz. More details can be found in [10] and in the paragraph 2.5.

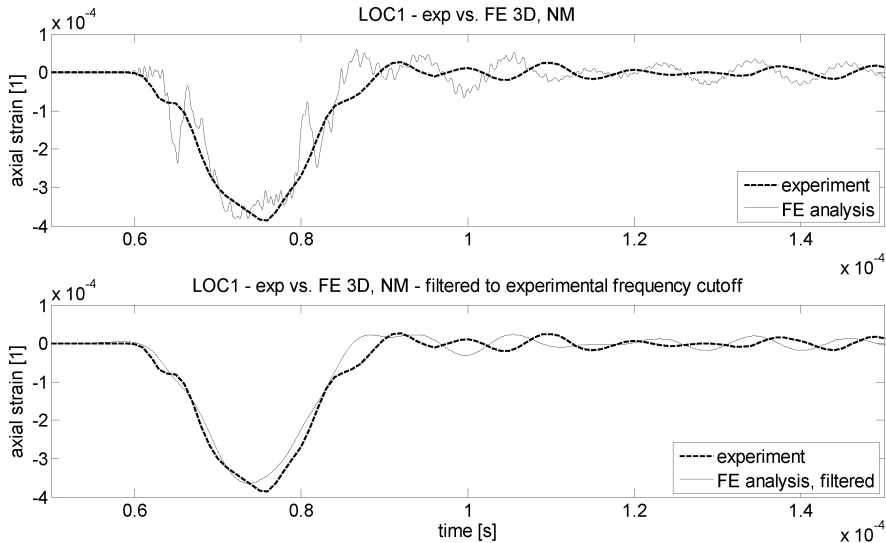


Fig.6: Comparison of experimental signal with raw and filtered FE data

2.5. Study case 4 – mesh refinement and frequency analysis of axisymmetric elements

The results presented in Fig. 6 show that the FE signal contains a greater contribution of high-frequency components. Among other things, this is due to the fact that the FE sampling rate, corresponding to the timestep used, is 10 MHz, which is the value ten times greater than that in the experiment.

In the lower part of Fig. 6 the experimental data are compared with FE data that were subjected to a filtering process with the upper cut-off frequency value being equal to that of experiment, i.e. 0.1 MHz. The Butterworth second order digital filter, as described in [14], was used. The agreement might be more plausible to naked eyes but not fully satisfying, because it was reached at the expense of filtering-out high frequency components from the FE signal, which the experiment, as it was conceived, could not register.

Evidently, a part of the high frequency contents in the experimental signal is missing. On the other hand it is known that the highest frequencies of the FE signal are corrupted due to time and space discretization side-effects. See [13].

And this leads to a question. That is, up to which frequency limit is the FE approach trustworthy?

We know that FE method is a model of continuum. The continuum – also a model – being based on the continuity hypothesis, disregards the corpuscular structure of matter.

It is assumed that matter within the observed specimen is distributed continuously and its properties do not depend on the specimen size. Quantities describing the continuum behavior are expressed as continuous functions of time and space. It is known, see [2], that such a conceived continuum has no upper frequency limit. To find a ‘meaningful’ frequency limit of FE model, which is of discrete – not continuous – nature, one might pursue the following heuristic reasoning.

Imagine a uniform finite element mesh with a characteristic element size, say h . Trying to safely ‘grasp’ a harmonic component (having the wavelength λ) by this element size we require that at least five-element length fits the wavelength. This leads to $\lambda = 5h$. What is the frequency of this harmonics? Taking a typical wave speed value in steel of about $c = 5000$ m/s and realizing that $\lambda = cT$ and $f = 1/T$, we get the sought-after ‘frequency limit’ in the form $f = c/(5h)$. For a one-millimeter element we get $f = 5000/(5 \times 0.001) = 1 \times 10^6$ Hz = 1 MHz. Let’s call it the **five-element frequency**, denoting it $f_{5\text{elem}}$ in the text.

Observing the original (or raw) FE signal in Fig. 6 we may notice its three significant characteristics. First, the negative peak representing the input rectangular pulse, as it was changed on its way from the loading face of the tube to the measurement location; second, the slow frequency variation of the tail of the signal and finally the high frequency components superimposed on the signal everywhere.

To estimate the low frequencies, appearing in the signal, let’s consider the lowest radial frequency of the unsupported infinitely long thin shell of the radius r . In [21] there is derived the formula

$$f = \frac{1}{2\pi r} \sqrt{\frac{E}{\rho} \frac{1 - \mu}{(1 + \mu)(1 - 2\mu)}},$$

which when applied to our case gives the value of 93 kHz. Due to the corresponding mode of vibration, let’s call this frequency the lowest **breathing frequency**.

The faster frequency appearing in time distributions of displacements and strains is called the **zig-zag frequency** in the text.

For the zig-zag frequency estimation let’s pursue the following reasoning.

According to Huygens’ Principle each point on the surface being hit by a wave is a source of two kinds of waves – the longitudinal and transversal (shear) waves, respectively [3].

At the beginning of the loading process the frequencies of evoked waves can be crudely estimated the following way. Each type of wave, being emanated from the outer surface, propagates through the tube thickness, is reflected from the inner surface, and hits the outer surface after the time interval

$$t_L = \frac{2s}{c_L}, \quad t_S = \frac{2s}{c_T},$$

where the tube thickness is denoted by s . The process is repeated. The corresponding estimates of frequencies of S- and L-waves hitting the outer surface are

$$f_L = \frac{1}{t_L}, \quad f_S = \frac{1}{t_S}.$$

Considering the given geometry and material properties the numerical values for these frequencies are

$$f_L = 0.93 \text{ MHz}, \quad f_S = 0.54 \text{ MHz}.$$

In the text we will call them **zig-zag frequencies** with attributes L (for longitudinal waves) and with S (for shear waves) respectively.

The case we are dealing with is three-dimensional even if its axial dimension is predominant and the thickness of the tube is rather small comparing to its axial length. Also the applied loading is rather mild – meaning that the time length of the pulse is relatively long with respect to time needed for a wave to pass through the overall length of the tube. Still, in reality there is a fully 3D wave motion pattern appearing within the tube cross section that is dutifully detected by the FE modeling we are employing.

To analyze the frequency contents of the signal and relate it to that of the loading pulse, let's employ the Fourier transform treatment using the Matlab Transfer Function Estimate, providing the transfer function of the system with the loading pulse as input, and the FE radial displacements, 'measured' at the outer corner node of the impacted face, Fig. 1, as the output, using the Welch's averaged periodogram method as defined in [27].

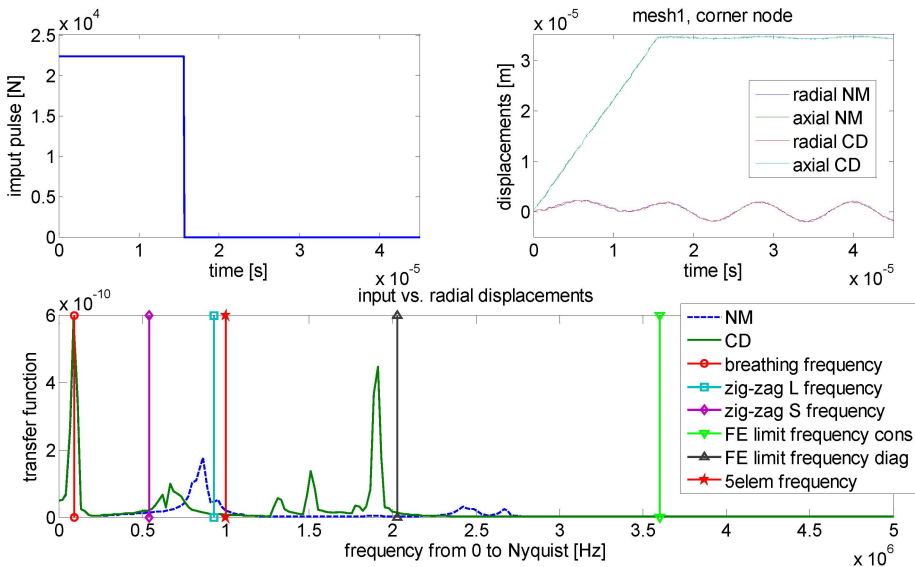


Fig.7: Transfer function for mesh1, NM vs. CD, limit frequencies

In the upper part of Fig.7 there are shown the time distributions of the loading pulse expressed as the loading forces computed from the loading pressure applied on the impact face (input signal) and those of radial and axial displacements (output signal), for the outer corner node of the impacted face of mesh1, as functions of time both for NM and CD time integration operators. In the lower part of Fig.7 the transfer functions for NM and CD operators are shown together with limit frequencies estimated before. In this case the presented transfer function, as computed by Matlab [27], is the cross spectrum of input signal (loading) and output signal (radial displacements) divided by the power spectrum of the input signal. The dimension of the transfer function depends on dimensions of input and output signals, does not bring a significant piece of information and is not thus presented in figures. The plotted frequency range is from 0 to the Nyquist frequency. See [26], [27]. The first peak perfectly coincides with the lowest breathing frequency. The subsequent peaks (different for NM and CD) are well positioned within the interval of frequencies for S- and L-zig-zag

waves. The 5-element frequency, together with largest eigenfrequencies stemming from the solution of the generalized eigenvalue problem are plotted for a comparison as well. They are obtained from the solution of $\mathbf{K}\mathbf{V} = \mathbf{M}\mathbf{V}\mathbf{\Lambda}$, where \mathbf{K} , \mathbf{M} are global stiffness and mass matrices; \mathbf{V} , $\mathbf{\Lambda}$ are modal matrix and diagonal matrix of eigenvalues, both for consistent and diagonal mass formulations. In Fig. 7 and 8 they are denoted FE_limit_frequency_diag and FE_limit_frequency_cons respectively.

There are clearly visible high-frequency suspicious peaks for the CD transfer function of radial displacements which do not have their counterparts in the NM spectrum.

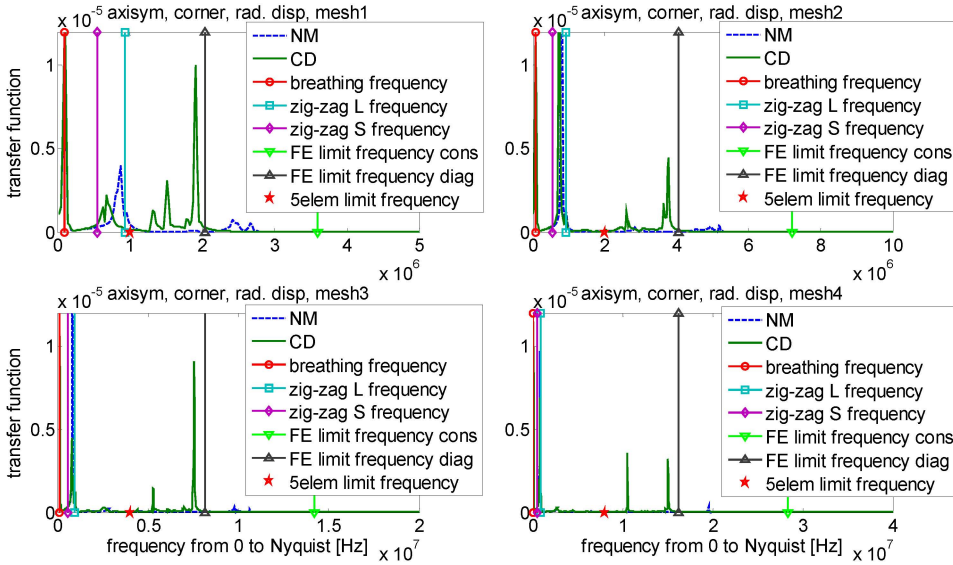


Fig.8: Transfer functions for different meshes from 0 to Nyquist

Fig. 8 summarizes the transfer function results for all four the analyzed meshes, i.e. for mesh1 to mesh4 – each consecutive mesh being twice as fine as the previous one – for the full range of frequencies (from 0 to Nyquist). The input pulse is normalized to its maximum value. Let’s concentrate on positions of suspicious peaks – outside of the expected ‘good’ frequency intervals and expressed in dimensionless frequencies $f^* = f/f_{\text{Nyquist}}$. They are identical for all the analyzed meshes.

Observing the transfer function spectra for mesh1 to mesh4 we claim that the vibration modes (detected by means of FE analysis) with frequencies higher than $f_{5\text{elem}}$ are numerical artifacts. It is worth noticing that they are substantially more pronounced for the CD operator.

The ‘fundamental’ frequencies embedded in response of the tube, we are interested in, are at the beginning of the spectrum as shown in the transfer function results in Fig. 9 – this time plotted within a shorter frequency range limited to 0 to 2 MHz.

Observing Fig. 9 one should notice the subsequent ‘convergence’ of CD and NM peaks within the zig-zag frequency interval. The natural explanation is that with the finer meshsize, and with the correspondingly smaller timestep, both methods operate in ‘good’ frequency intervals where their spatial and temporal discretization errors are insignificant.

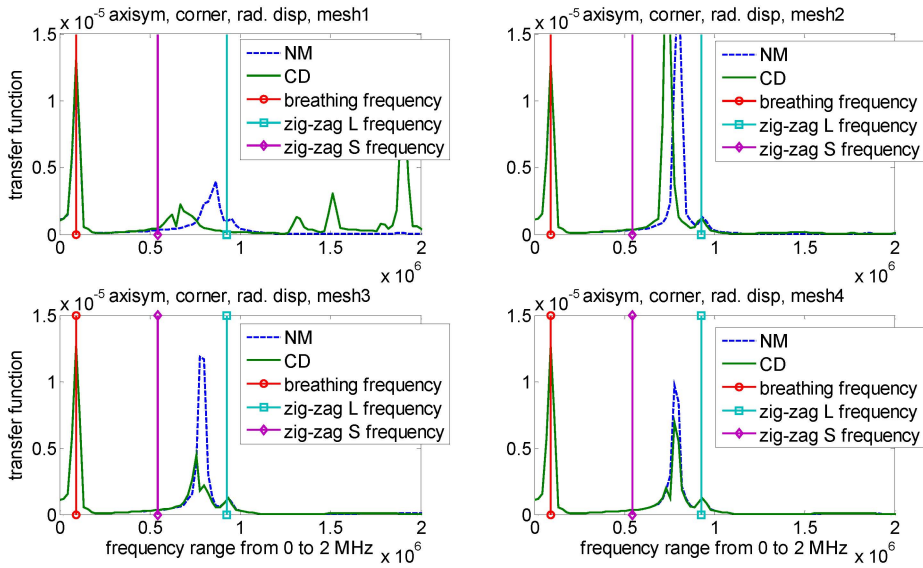


Fig.9: Transfer functions for different meshes from 0 to 2 MHz

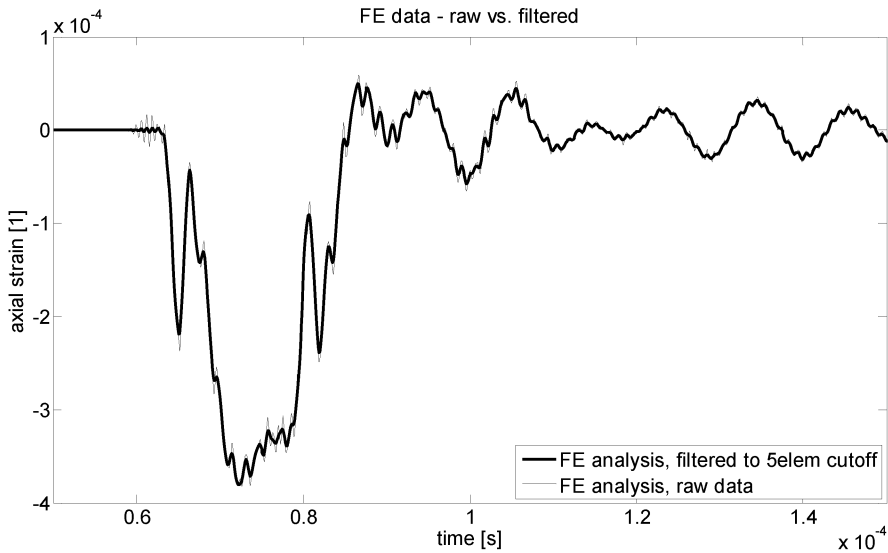


Fig.10: FE raw signal compared to that in which the frequencies higher than five-element ones were filtered out

The presented transfer spectra for four studied meshes show

- a distinct indication of the breathing and zig-zag frequencies,
- the ‘convergence’ of CD and NM responses,
- subsequent disappearance of ‘false’ CD responses and
- that the ‘dubious’ CD frequency peaks do not have their counterparts in NM responses.

What remains to be compared is the ‘raw’ FE signal with that the frequencies higher than the five-element frequency were filtered out. The results for the ‘raw’ and filtered FE

signals, for the mesh1 and the NM operator with consistent mass matrix, are presented in Fig. 10.

In future these FE results might be confirmed by a more sophisticated experiment having a lower observational threshold, a higher sampling rate and also a higher frequency amplifier cut-off.

2.6. Study case 5 – assessment of ‘close’ solutions by statistical tools for results obtained by NM and CD operators for different time and space discretizations

The variance, covariance and correlation coefficients, see [27], could be used as quantitative measures of quality of agreement between different measurements or solutions. Especially the correlation coefficient is a good measure for the quality of ‘sameness’ of two solutions or measurements. Of course closer are the results to unity – the better.

The **variance** of a signal is the **standard deviation** squared. It measures how much the entries of the signal (individual samples, variables) vary. The **covariance**, on the other hand, measures, how much two (or more) signals vary together. The diagonal entries of covariance matrix indicate how the signal varies with respect to itself – so its value is equal to variance of that signal. The **correlation** indicates the strength and direction of a linear relationship between two (or more) variables. The correlation refers to the departure of two (or more) variables from linear independence. For more details see [14], [22].

Now, we will concentrate on assessment of radial displacements of the corner node of the impacted face as obtained by four different meshes, i.e. mesh1 to mesh4 and by the Newmark (NM) and central difference (CD) time operators. The data are presented in Fig. 11. Only the beginning of the studied time range is depicted.

The finer meshes are processed with proportionally smaller timesteps, so the lengths of data belonging to individual meshes for the same time interval are different and cannot be

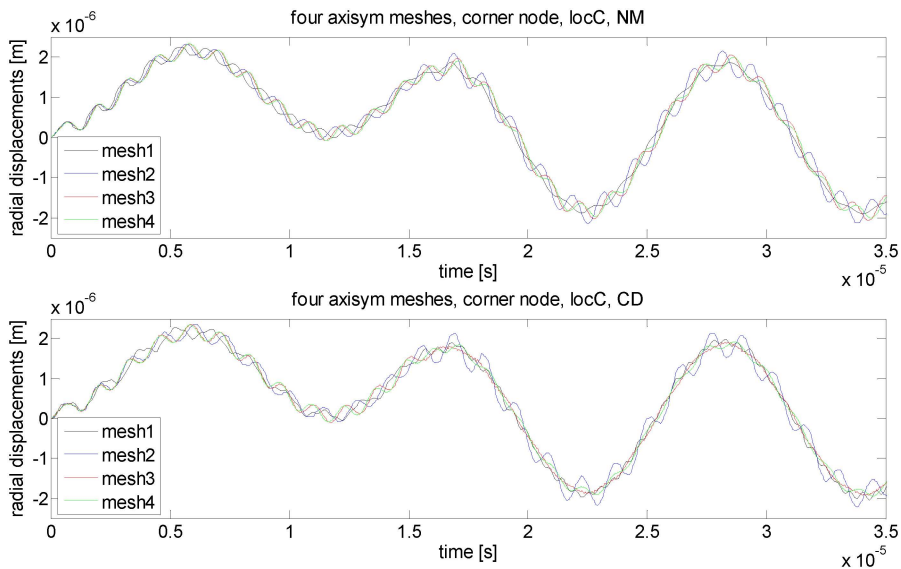


Fig.11: Radial displacements of the corner node, four axisymmetric meshes, NM and CD

directly compared, one against another, by means of statistical tools as variance, covariance and correlation.

To remove this hindrance the coarse mesh data are filled in by linearly interpolated values which are inserted in such a way that all the data samples are of the same length equal to that of the finest mesh, i.e. mesh4.

The variance and covariance for mesh1 to mesh4 data, obtained by FE analysis, are presented in Fig. 12.

Variance shows how noisy is the signal. For mesh1 and for mesh2 the variances of CD data (stars) are substantially greater (i.e. the signal is noisier) than those of NM data (circles). For mesh3 and mesh4 it is just the opposite but they have a tendency to converge. This means that mesh3 and mesh4 data seem to be almost insensitive both to mesh density and the choice of the integrating operator – under these conditions the method of computation becomes robust, i.e. independent (of course within the scope of employed method and the presented example) of the computational approach. Covariance results (diamond markers in Fig. 12) indicate how the NM results differ from the CD results for individual meshes.

The reasoning based on statistical tools, together with conclusions stemming from the frequency analysis presented above, indicate that we might be quite satisfied with precision provided by the finest mesh regardless of the time integration operator used. Temporal and spatial dispersion effects are negligible. Assembling, however, the tube of mesh4 elements ($h = 1/8$ mm) is for practical engineering purposes too expensive. After all, we have to rely on results obtained by means of the coarse mesh (mesh1). Still, these results guarantee that within the 1 MHz frequency interval, i.e. within the 5-element frequency range, the high-frequency zig-zag modes, appearing in FE computed strains, are to be believed.

Authors are aware of the fact that a relatively small number of cases was treated statistically in this paper. But the main motivation for the presented statistical treatment was to suggest a methodology procedure allowing the quantitative assessment of ‘close’ solutions replacing thus the commonly used qualitative assertions based on the optical observations of results leading to statements as *the agreement is good within the line thickness*.

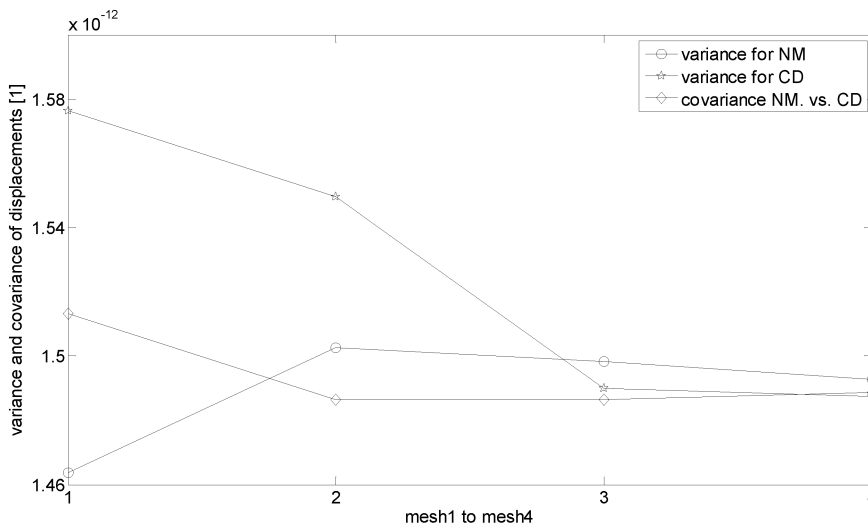


Fig.12: Statistical assessment of ‘close’ solutions

Of course the mentioned statistical tool are not omnipotent. They might be wrongly interpreted in cases when one time signal is a multiple of another, or when two signals are shifted in value by a constant. But these cases are easily excluded from the considerations on the bases of engineering judgement.

3. Conclusions

The FE analysis is a robust tool giving reliable results with a satisfactory engineering precision in standard tasks of continuum mechanics. Nevertheless, employing the FE method in cases on borders of their applicability is tricky and obtained results have to be treated with utmost care, since they might be profoundly influenced by intricacies of finite element technology. It should be emphasized, however, that testing the methods in the vicinity of borders of their applicability we do not want to discredit them, on the contrary, the more precise knowledge of their imperfections makes us – users – more confident in them.

Modeling the nature should be independent of employed tools, means and methods. Unfortunately plethora of numerical procedures, of which the FE modeling is built up, gives the FE user a chance to meddle with many optional parameters that might influence the results significantly. Specifically, the modeling of fast transient phenomena in solid mechanics by FE analysis can be provided by many different approaches based on a wide choice of element types with different admissible quadrature procedures, employing different time step operators, different timesteps, mass matrix formulations, details of mesh assembling, just to name a few.

Generally, the questions concerning the credibility of FE modeling, could only be answered indirectly – comparing the results of the same task obtained by different approaches, as using different time step operators, coarse and subsequently refined meshes, analyzing them using Fourier analysis, checking the conditions of logical consistency, etc.

The presented study resulted from the previous extensive treatment of stress waves propagating through a solid cylinder with a spiral groove [23] and from considerations devoted to comparison of results of experimental and FE analysis of stress waves in thin shells, see [17], and can viewed as a preliminary study dedicated to experimental and FE treatment of stress waves in thin tubes, see [10]. The authors believe that the analyzed results might contribute to intuitive understanding of the scope of validity of FE models in transient dynamics.

The role of the experiment, as a tool for the ultimate verification of the mathematical modeling, is indispensable but not always at our disposal when needed. Nevertheless the experiment, as well as in FE analysis, is biased by observational thresholds, systematic errors, frequency limitations, etc.

So in most cases the credibility of our FE computations has to rely on model self-checking accompanied by a profound judgment of acceptability of employed theories, hypothesizes and models.

Acknowledgement

The support of the Grant 1ET400760509 of the Academy of Sciences of the Czech Republic and that of the Solid mechanics Department of the Ångström Laboratory, Uppsala University, Sweden is highly appreciated.

References

- [1] Todhunter I., Pearson K.: A history of elasticity and of the strength of material, Dover Publications, New York, 1960, Initially appeared in 1886
- [2] Love A.E.H.: A Treatise on the Mathematical Theory of Elasticity, (First edition 1892), New York, Dover Publications 1944
- [3] Brepta R., Okrouhlík M., Valeš F.: Wave and impact phenomena in solids and methods of solutions, (in Czech: Vlnové a rázové děje v pevných tělesech a metody jejich řešení), Studie ČSAV No. 16, Academia, Praha 1985
- [4] Červ J., Valeš F., Volek J., Landa M.: Wave propagation in plates under transverse impact loading, In: International congress on sound and vibration: ICSV9, Orlando, University of Central Florida, 2002, 1–8, Proceedings of the International Congress on Sound and Vibration, Orlando, 2002
- [5] Stein E., de Borst R., Hughes T.J.R (Editors): Encyclopedia of Computational Science, John Wiley, Chichester, 2004
- [6] Duncan W.J., Collar A.R.: A method for the solution of oscillatory problems by matrices, Phil. Mag. Series 7, 17, pp.865, 1934
- [7] Duncan W.J., Collar A.R.: Matrices applied to the motions of damped systems, Phil. Mag. Series 7, 19, pp.197, 1935
- [8] Felippa A.C.: A historical outline of matrix structural analysis: A play in three acts. Computers and Structures, 79, pp.1313–1324, 2001, Also Report CU-CAS-00-14, June 2000, University of Colorado, Boulder, CO, 80309-0429, USA
- [9] Flüge S. (editor): Encyclopedia of Physics. Vol. III. Principles of Classical Mechanics and Field Theory, Springer Verlag, Berlin, 1960
- [10] Okrouhlík M., Pták S.: FE and experimental study of axially induced shear stress waves in a tube with spiral slots. Part 1. Research Report of the Institute of Thermomechanics, Z 1417/2008, Prague, 2008
- [11] Ueberhuber Ch.W.: Numerical Computation, Springer, Berlin, 1997
- [12] Papadrakakis M. (editor): Solving Large Scale Problems in Mechanics, John Wiley, Chichester, 1993
- [13] Okrouhlík M. (editor): Mechanics of Contact Impact, Applied Mechanics Review, Vol.47, No. 2, February 1994
- [14] Marc manuals, MSC Software Corporation, 2 MacArthur Place, Santa Ana, CA 92707 USA, www.mscsoftware.com
- [15] Ansys manuals, <http://www.ansys.com>
- [16] Belytschko T., Liu W.K., Moran B.: Nonlinear Finite Elements for Continua and Structures, John Wiley, Chichester, 2000
- [17] Okrouhlík M., Pták S.: Assessment of experiment by finite element analysis: Comparison, self-check and remedy, Strojnícky časopis, Vol. 56, 2005, No. 1
- [18] Bathe K.-J.: Finite Element Procedures, Prentice-Hall, Englewood Cliffs, New Jersey, 1996
- [19] Kahan W.: IEEE Standard 754 for Binary Floating-Point Arithmetic, Lecture Notes on the Status of IEEE 754, Elect. Eng. & Computer Science, UCLA, Berkeley, 1997
- [20] Kolsky, H.: Stress Waves in Solids, Clarendon Press, Oxford, 1993
- [21] Blevins R.D.: Formulas for mode frequencies and mode shape, Krieger Publishing Company, Malaba, Florida, 1998
- [22] Press W.H., Teukolsky S.A., Vetterling W.T., Flannery B.P.: Numerical recipes: The art of scientific computing, Cambridge: Cambridge University Press, 1986
- [23] Okrouhlík M., Pták S.: Numerical Modeling of Axially Impacted Rod with a Spiral Groove, Inženýrská Mechanika, Vol. 10, No. 5, pp. 359–374, 2003
- [24] PMD manual. Version f77.9, VAMET/Institute of Thermomechanics, 2003
- [25] Dyna manuals, www.dynasupport.com/support/tutorial/users.guide.
- [26] Doyle J.F.: Modern Experimental Stress Analysis, John Wiley, Chichester, 2004
- [27] Matlab Signal Processing Toolbox, www.mathworks.com.

Received in editor's office: August 11, 2008

Approved for publishing: November 7, 2008